Quarterly Technical Report

Selected Energy Epitaxial Deposition and Low Energy Electron Microscopy of AlN, GaN and SiC Thin Films

Supported under Grant #N00014-95-1-0122
Office of the Chief of Naval Research
Report for the period 1/1/97–3/31/97

R. F. Davis, H. H. Lamb† and I. S. T. Tsong*,
E. Bauer*, E. Chen†, R. Chilukuri†, R. B. Doak*, J. L. Edwards*,
N. Freed*, J. Fritsch*, D. C. Jordan*, A. Michel, M. Meloni*,
A. Pavlovska*, K. E. Schmidt*, V. Torres*, and S. Zhang
Materials Science and Engineering Department
†Chemical Engineering
North Carolina State University
Campus Box 7907
Raleigh, NC 27695-7907
and
*Department of Physics and Astronomy
Arizona State University
Tempe, AZ 85287-1504

March, 1997

REPORT DOCUMENTATION PAGE

Form Approved
OMB No. 0704-0188

1. AGENCY USE ONLY *(Leave blank)*	2. REPORT DATE	3. REPORT TYPE AND DATES COVERED
	March, 1997	Quarterly Technical 1/1/97–3/31/97

4. TITLE AND SUBTITLE
Selected Energy Epitaxial Deposition and Low Energy Electron Microscopy of AlN, GaN, and SiC Thin Films

5. FUNDING NUMBERS
1213801---01
312
N00179
N66020
4B855

6. AUTHOR(S)
R. F. Davis, H. H. Lamb and I. S. T. Tsong

7. PERFORMING ORGANIZATION NAME(S) AND ADDRESS(ES)
North Carolina State University
Hillsborough Street
Raleigh, NC 27695

8. PERFORMING ORGANIZATION REPORT NUMBER
N00014-95-1-0122

9. SPONSORING/MONITORING AGENCY NAMES(S) AND ADDRESS(ES)
Sponsoring: ONR, Code 312, 800 N. Quincy, Arlington, VA 22217-5660
Monitoring: Administrative Contracting Officer, Regional Office Atlanta
Regional Office Atlanta, 101 Marietta Tower, Suite 2805
101 Marietta Street
Atlanta, GA 30323-0008

10. SPONSORING/MONITORING AGENCY REPORT NUMBER

11. SUPPLEMENTARY NOTES

12a. DISTRIBUTION/AVAILABILITY STATEMENT
Approved for Public Release; Distribution Unlimited

12b. DISTRIBUTION CODE

13. ABSTRACT ***(Maximum 200 words)***

The total energies for various p(2×2) geometries of GaN and AlN(0001) have been computed. Vacancy structures were the most stable configurations for the anion- and cation-terminated surfaces. In metal rich growth conditions, the calculations favored the adsorption of metal atoms on the cation terminated surface; the adsorption of H stabilized the N-terminated surface in the presence of H. Films of AlN and GaN were grown on Si(111) and off-axis 6H-SiC(0001) substrates under real-time observations in the LEEM. The metals were deposited using evaporative sources; N-atoms were obtained via RF plasma source. Additional homoepitaxial growth of GaN films at typical rate of 20 nm/h was achieved between 600 and 700°C using TEG-seeded and NH_3 seeded supersonic beams. AFM revealed faceted growth surfaces. XPS indicated the N/Ga ratio at the growth surface approached unity with an increase in the ammonia-to-TEG flux ratio. TEM analysis of AlN films and subsequently deposited GaN layers grown using evaporated metals and NH_3-seeded He supersonic molecular beams showed the latter to be epitaxial with a thickness of ≈0.1 μm and a defect density on the order of 2×10^{10} cm^{-2}. The AlN buffer layers contained about an order of magnitude higher defect density relative to GaN. N incorporation efficiencies greater than 41% are achieved using NH_3 kinetic energies of 0.40 eV during GaN film growth. A compact (25 cm long by 10 cm diameter) arc-heated supersonic nozzle has been constructed, tested and used to generate high intensity beams of both atomic nitrogen (N) and electronically-excited molecular nitrogen (N'_2). It has now been run successfully for several hours in both an arc-discharge mode (generating N atoms) as well as a glow-discharge mode generating (N'_2). The supersonic free-jet extracted from this "external arc" had a fractional dissociation of (84±9)% as measured with a mass spectrometer. The arc temperature, taken from throughput measurements, is indicated to be (7590±910)K. Mass-selected Ga^+ ions have been extracted from a Colutron source producing beams at ≈14 eV with a FWHM of ~1 eV.

14. SUBJECT TERMS
gallium nitride, GaN, aluminum nitride, AlN, supersonic jets, low energy electron microscopy, LEEM, calculations, adsorption, RF plasma, homoepitaxial, supersonic beams, nozzle, atomic nitrogen, molecular nitrogen, glow discharge, Colutron

15. NUMBER OF PAGES
30

16. PRICE CODE

17. SECURITY CLASSIFICATION OF REPORT	18. SECURITY CLASSIFICATION OF THIS PAGE	19. SECURITY CLASSIFICATION OF ABSTRACT	20. LIMITATION OF ABSTRACT
UNCLAS	UNCLAS	UNCLAS	SAR

Table of Contents

I. Introduction

The realized and potential electronic applications of AlN, GaN and SiC are well known. Moreover, a continuous range of solid solutions and pseudomorphic heterostructures of controlled periodicities and tunable bandgaps from 2.3 eV (3C-SiC) to 6.3 eV (AlN) have been produced at North Carolina State University (NCSU) and elsewhere in the GaN-AlN and AlN-SiC systems. The wide bandgaps of these materials and their strong atomic bonding have allowed the fabrication of high-power, high-frequency and high-temperature devices. However, the high vapor pressures of N and Si in the nitrides and SiC, respectively, force the use of low deposition temperatures with resultant inefficient chemisorption and reduced surface diffusion rates. The use of these low temperatures also increases the probability of the uncontrolled introduction of impurities as well as point, line and planar defects which are likely to be electrically active. An effective method must be found to routinely produce intrinsic epitaxial films of AlN, GaN and SiC having low defect densities.

Recently, Ceyer [1, 2] has demonstrated that the barrier to dissociative chemisorption of a reactant upon collision with a surface can be overcome by the translational energy of the incident molecule. Ceyer's explanation for this process is based upon a potential energy diagram (Fig. 1) similar to that given by classical transition-state theory (or activated-complex theory) in chemical kinetics. The dotted and dashed lines in Fig. 1 show, respectively, the potential wells for molecular physisorption and dissociative chemisorption onto the surface. In general, there will be an energy barrier to overcome for the atoms of the physisorbed molecule to dissociate and chemically bond to the surface. Depending upon the equilibrium positions and well depths of the physisorbed and chemisorbed states, the energy of the transition state E^* can be less than zero or greater than zero. In the former case, the reaction proceeds spontaneously. In the latter case, the molecule will never proceed from the physisorbed state (the precursor state) to the chemisorbed state unless an additional source of energy can be drawn upon to surmount the barrier. This energy can only come from either (1) the thermal energy of the surface, (2) stored internal energy (rotational and vibrational) of the molecule, or (3) the incident translational kinetic energy of the molecule. Conversion of translational kinetic energy into the required potential energy is the most efficient of these processes. Moreover, by adjusting the kinetic energy, Ei, of the incoming molecule, it is possible to turn off the reaction ($Ei < E^*$), to tailor the reaction to just proceed ($Ei = E^*$), or to set the amount of excess energy to be released ($Ei > E^*$). The thrust of the present research is to employ these attributes of the beam translational energy to tune the reaction chemistry for wide bandgap semiconductor epitaxial growth.

The transition state, E^*, is essentially the activation energy for dissociation and chemisorption of the incident molecules. Its exact magnitude is unknown, but is most certainly

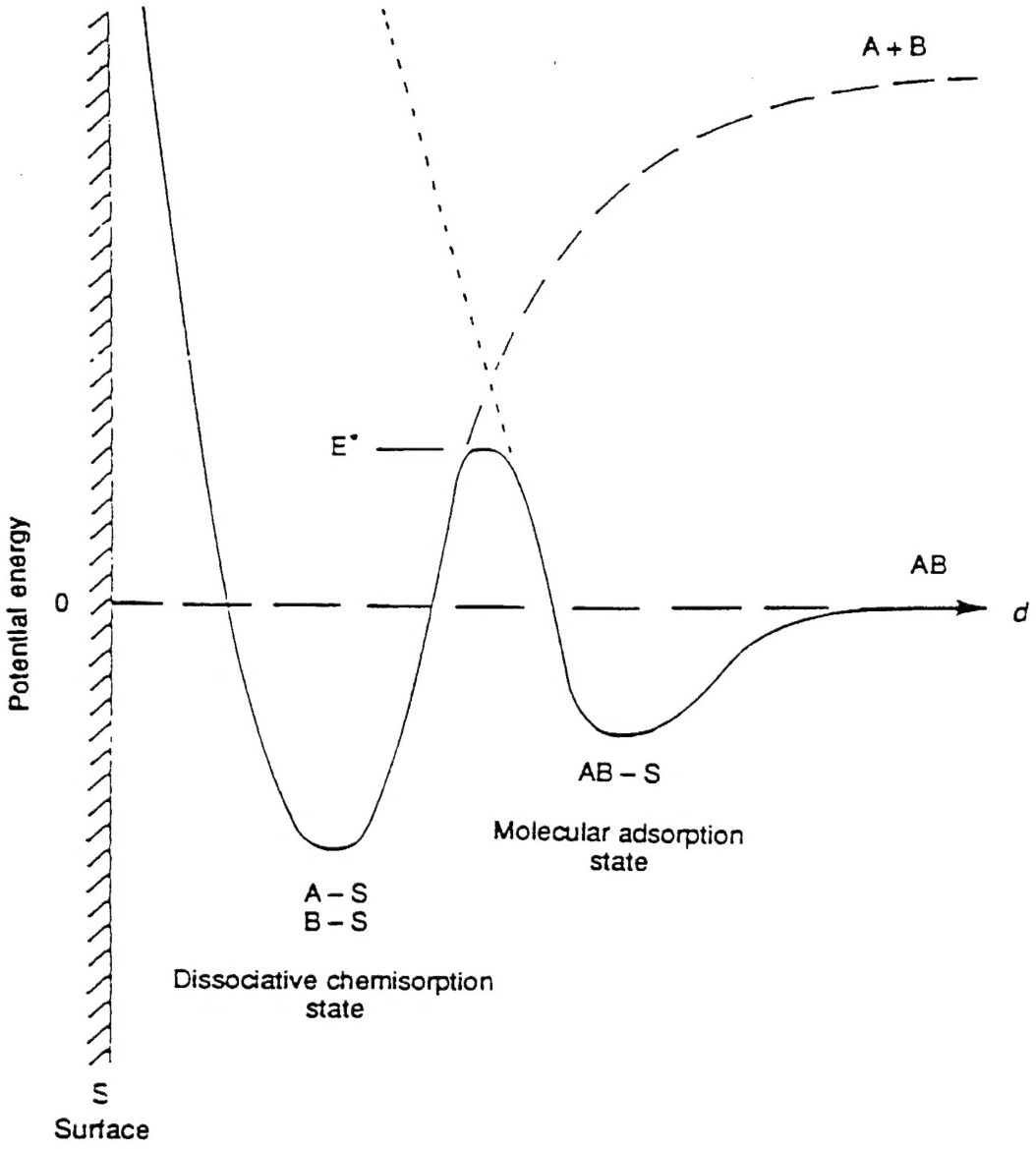

Figure 1. Schematic potential energy diagram of an activated surface reaction involving a molecularly physisorbed precursor state [from Ref. 1].

lower than the dissociation energy of the free molecule. It does not necessarily follow, however, that any kinetic energy above E* will promote high-quality epitaxial growth of GaN. One must take into consideration another energy threshold, Ed, beyond which the kinetic energy of the incident flux will cause damage to the epitaxial film being synthesized. A typical Ed threshold value is approximately five times the bandgap of the crystal and in the case of GaN, Ed ≈18 eV.

From the above consideration, it is clear that the key to high quality epitaxial growth is to be able to tune the energy of the incoming flux species over a range of energies defined by the window between E* and Ed. Since the window is quite restrictive, i.e. 1-20 eV, it is essential

that the energy spread of the flux species must be small, i.e. the flux species should ideally be monoenergetic. To this end, we employ Selected Energy Epitaxial Deposition (SEED) systems for the growth of AlN, GaN and SiC wide bandgap semiconductors. The SEED systems are of two types: (1) a seeded-beam supersonic free-jet (SSJ) and (2) a dual ion-beam Colutron. Both these SEED systems have the desirable property of a narrow energy spread of ≤ 1 eV.

Epitaxial growth using the seeded-beam SSJ involves a close collaboration between investigators at NCSU and Arizona State University (ASU). At ASU, the SSJ is interfaced directly into a low-energy electron microscope (LEEM) for the conduct of *in situ* studies of the nucleation and growth of epitaxial layers; while at NCSU, the SSJ systems are used to grow device-quality AlN, GaN and SiC for real applications. Exchanges in personnel (students) and information between the two groups ensures the achievement of desired results. The additional thin film growth experiments using dual-beam Colutrons and the theoretical studies referred to in this report are primarily conducted at ASU.

The research conducted in this reporting period and described in the following sections has been concerned with (1) *ab initio* calculations of the structure and growth properties of GaN and AlN, (2) the growth of stoichiometric and smooth AlN and/or GaN thin films on Si(111) and/or 6H-SiC(0001) substrates in the LEEM and in a specially constructed growth chamber using two different growth techniques, (3) the characterization of the III-nitride films via TEM and XPS, (4) the use of an arc-heated supersonic free jet of N atoms for the growth of GaN, AlN and InN films and (5) the extraction of mass selected, essentially monoenergetic ($\approx$14 eV) and chemically pure Ga^+ ion beams with a FWHM of $\approx$1 eV from a second Colutron source. The following individual sections detail the procedures, results, discussions of these results, conclusions and plans for future research. Each subsection is self-contained with its own figures, tables and references.

1. S. T. Ceyer, Langmuir 6, 82 (1990).
2. S. T. Ceyer, Science 249, 133 (1990).

II. *Ab initio* Calculation of the Structure and the Growth Properties of the III-V Nitrides

A. Introduction

Thin GaN and AlN films are primarily grown on the hexagonal surfaces of sapphire and 6H-SiC by means of molecular beam epitaxy (MBE) or metal-organic chemical-vapor deposition (MOCVD) [1-5]. Although many different experiments have been performed to monitor the epitaxial processes and to characterize the resulting morphology of the thin films, the growth phase of wurtzite AlN and GaN has not been completely understood. By means of low-energy electron diffraction (LEED) or reflection high-energy electron diffraction (RHEED), sharp $p(1\times1)$ patterns have been reported for well-ordered surfaces [1, 6, 7], while some MBE-grown nitride films exhibit a $p(2\times2)$ reconstruction [5, 8, 9]. Other experiments provide indication for higher-order reconstructions like $p(2\times1)$, $p(2\times3)$ or $p(5\times5)$ [10]. In a recent scanning-tunneling microscopy experiment, line-shaped and oval defects have been reported for GaN(0001) and attributed to vacancies [11].

The large variety of experimental observations reported in Refs. [1, 5-11] can only partially be explained by the results obtained from the *ab initio* calculations of Refs. [12-14]. Specifically, the influence of hydrogen on the growth phase observed by experiment [1] has not been considered in the previous theoretical work.

This report focuses on the systematic analysis of a large variety of surface structures examined for the hexagonal surfaces of wurtzite phase GaN and AlN by means of molecular dynamics simulations using a fast *ab initio* multicenter tight-binding formalism applied to slab-supercell calculation.

B. Experimental Procedure

The energy differences between the reconstructions considered for one surface of the slabs were essentially independent on the reference configuration fixed on the other side of the films. First, results were summarized for the cation-terminated surface of GaN and AlN using a nitrogen-vacancy complex as reference configuration on the (0001) surface. Figure 1 compares the total energies per $p(2\times2)$ unit cell of the most important surface structures. The lowest-energy configuration was the cation vacancy labeled (a) which was lower by about 0.7 eV (0.3 eV) than the adsorption of nitrogen on the hollow site (b) of the (0001) surface of GaN (AlN). For the chemisorption of nitrogen, the H_3 site (b) was preferred above the T_4 position (e) by 4.0 eV (1.9 eV) in the case of GaN (AlN). The adsorption of a nitrogen atom changed the stoichiometry the same way the creation of a cation vacancy did since in both cases the number of cations in the surface bilayer was smaller by one compared to the number of anions. Consequently, the relative energy difference of the structures (a), (b), and (e) was independent of the chemical potential of the Group III atoms.

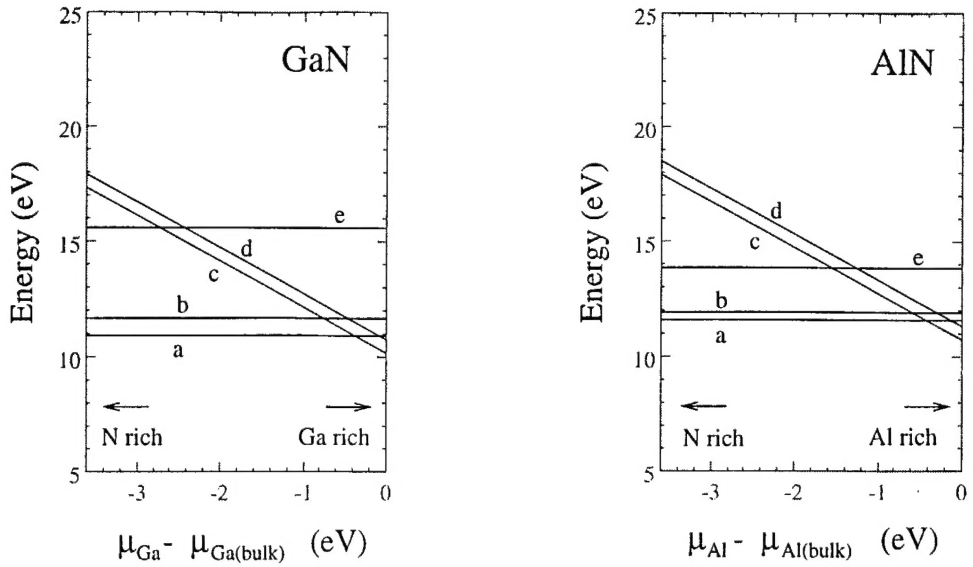

Figure 1. Comparison of the total energies per $p(2\times2)$ unit cell of the most important surface structures.

In contrast, the adsorption of Group III atoms involved more cations than anions in the surface region leading to relative energies that depended on the chemical potential of the metal atoms when compared to structures (a), (b), and (e). Hence, the metal-adatom T_4 configuration (c) was lower in energy than all other structures in a range of -0.4 eV $\leq \Delta\mu \leq$ 0.0 eV (-0.45 eV $\leq \Delta\mu \leq$ 0.0 eV) for the chemical potential of gallium (aluminum). The H_3 adsorption site (d) was less favorable by 0.6 eV for both compounds. This agreed significantly with the *ab initio* calculation of Ref. [12] which yielded the lowest energy for the adsorption of Group III atoms on the T_4 site of GaN(0001) in metal-rich conditions. In contrast with Ref. [12] but in agreement with the *ab initio* study of Di Felice [14], calculations slightly favored the cation vacancy above the adsorption of nitrogen on the hollow site.

For the different structures considered on the anion terminated GaN(000$\bar{1}$) and AlN(000$\bar{1}$) surface, results obtained with the cation vacancy as reference configuration on the cation terminated side of the slab supercells are summarized. Figure 2 displays the energies for the vacancy (a), the vacancy complex (b), the adsorption of a Group III atom on the H_3 (c) and the T_4 (d) site, as well as the adsorption of nitrogen on the T_4 position (e). The structures (a–d) were similar in stoichiometry with one nitrogen atom less per $p(2\times2)$ unit cell compared to the number of cations in the surface region. For both compounds, the energy order of the different structures was the same. In agreement with Ref. [12], the nitrogen vacancy was found to be more stable compared to adatom configurations. However, in the previous calculation, only the vacancy was considered. Particularly for AlN(000$\bar{1}$), the vacancy complex turned out to be lower in energy by 0.7 eV, while the energy difference was slightly smaller for GaN(0001) for which 0.3 eV was obtained.

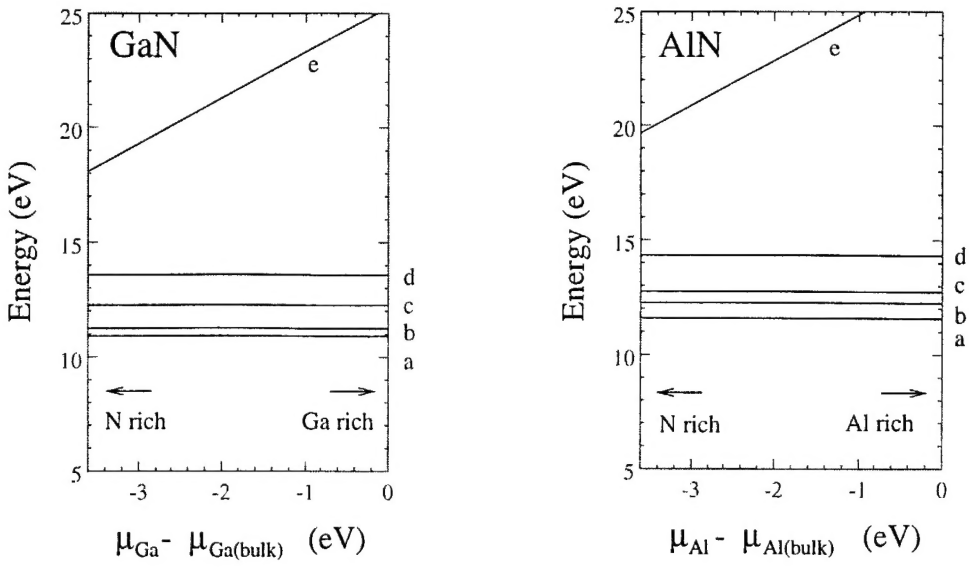

Figure 2. Energies for the vacancy (a), the vacancy complex (b), the adsorption of a Group III atom on the H_3 (c), the T_4 (d) site, and the adsorption of nitrogen on the T_4 position (e).

In the presence of hydrogen, Sung and co-workers reported the formation of hydrogen-adsorption layers on the flat GaN(0001) surface [1]. To examine to what extent hydrogen stabilizes the nitrogen terminated surfaces, the total energy was computed for a free ammonia molecule above the (0001) surface of GaN and AlN exhibiting one nitrogen vacancy per $p(2\times2)$ unit cell. The result was compared to the case in which the nitrogen atom of the ammonia molecule was incorporated into the vacancy while the hydrogen atoms saturated three of the four dangling bonds. This structure corresponded to the adsorption of 3/4 monolayer of hydrogen as suggested in Ref. [1]. Total energy calculation showed the adsorption system was lower in energy by 5.1 eV for GaN and 5.8 eV for AlN. Hence, incorporation of ammonia into the nitrogen terminated surface was highly exothermic in the presence of nitrogen vacancies.

C. Conclusions

In summary, several reconstructions have been investigated for the anion- and cation-terminated surface of GaN and AlN. The modification of the stoichiometry in the outermost layers eliminated the surface polarity and stabilized the surfaces. Depending on the chemical potentials of the bonding partners, different surface structures were found to be stable. Vacancy-structures on the nitrogen-terminated surface led to an exothermic incorporation of nitrogen and the formation of hydrogen overlayers in the presence of ammonia.

D. References

1. M. M. Sung, J. Ahn, V. Bykov, J. W. Rabalais, D. D . Koleske, and A. E. Wickenden, Phys. Rev. B **54**, 14652 (1996).

2. F. A. Ponce, C. G. Van de Walle, and J. E. Northrup, Phys. Rev. B **53**, 7473 (1996).
3. S. Strite and H. Morkoc, J. Vac. Sci. Technol. B **10(4)**, 1237 (1992).
4. S. Strite, in *Festkörperprobleme/Advances in Solid State Physics*, Vol. 34, ed. by R. Helbig, (Vieweg, Braunschweig, Wiesbaden, 1995), p. 29.
5. P. Hacke, G. Feuillet, H. Okumara and S. Yoshida, Appl. Phys. Lett. **69** (17), 2507 (1996).
6. G. V. M. Bermudez, R. Kaplan, M. A. Khan, and J.N. Kuznia, Phys. Rev. B **48** 2436 (1995)
7. M. A. Khan, J. N. Kaznia, D. T. Ohlson and R. Kaplan, J. Appl. Phys. **73**, 3108 (1993).
8. K. Iwata, H. Asahi, S. J. Ju, K. Asami, H. Fujita, M. Fushida, and S. Gonda, Jpn. J. Appl. Phys. **35**, L289 (1996).
9. M. E. Lin, S. Strite, A. Agarwal, A. Salvador, G. L. Zhou, N. Teraguchi, A. Rockett, and H. Morkoc, Appl. Phys. Lett. **62**, 707 (1993).
10. W. C. Hughes, W. H. Rowland, Jr., M. A. L. Johnson, S. Fujita, J. W. Cook, Jr., J. F. Schetzina, J. Ren, and J. A. Edmond, J. Vac. Sci. Technol. B **13**, 1571 (1995).
11. W. E. Packard, J. D. Dow, K. Doverspike, R. Kaplan, and R. Nicolaides, Journal of Materials Research **12**, 646 (1997); W. E. Packard, J. D. Dow, R. Nicolaides, K. Doverspike and R. Kaplan, Superlattices and Microstructures **20**, 145 (1996).
12. M. Buongiorno-Nardelli *et al.* (to be published)
13. R. B. Capaz H. Lim and J. D. Joannopoulos, Phys. Rev. B **51**, 17755 (1995).
14. R. Di Felice, J. E. Northrup, and J. Neugebauer, Phys. Rev. B **54**, R17351 (1996).

III. *In situ* LEEM Studies of the Growth of AlN and GaN on Si(111) and 6H-SiC(0001) using a RF Plasma Atomic Nitrogen Source

A. Introduction

In order to evaluate to what extent selected energy deposition improves the quality of epitaxial GaN and AlN layers, it is necessary to conduct comparative growth experiments with non-energy-selected beams. Previous *in situ* experiments with a thermal ammonia beam produced epitaxial AlN layers. Gallium nitride layers, however, could not be grown epitaxially because ammonia did not dissociate sufficiently at the temperatures at which Ga was sticking to the surface. As a consequence, it was decided to use an atomic nitrogen beam from a microwave discharge.

B. Experimental Procedure

The RF plasma atomic nitrogen source, an Oxford Applied Research CARS25 source on loan from the Deutsche Forschungsgemeinschaft, was mounted on the LEEM at the same angle of incidence as the future supersonic ammonia beam source, i.e. 16°. Evaporative cells of Al and Ga were also mounted at the same incident angle. Beams with sufficiently high atomic nitrogen concentration could only be obtained with flow rates at pressures between 6×10^{-6} and 2×10^{-5} Torr in the specimen chamber. These pressures were considerably higher than previous LEEM operating pressures. However, they turned out not to be detrimental to the imaging process. The N flux density at the specimen was not determined. The flux densities of the Al and Ga beams were in general in the range 2 - 5×10^{14} atoms/cm^{2}min which led to metal flux-limited growth. In the experiments on SiC(0001), the Ga flux density was increased to 4×10^{15} atoms/cm^{2}min resulting in N flux-limited growth. Standard cleaning procedures were used for the Si(111) surfaces. The SiC(111) surfaces were cleaned by heating to increasingly higher temperatures up to the onset of graphitization.

C. Results

Growth on Si(111) Substrates. Two starting conditions for the growth on Si(111) were used: (i) a surface covered with 1 ML Al as characterized by the Al"(7×7)" pattern and (ii) surfaces covered with a monolayer of silicon nitride as characterized by the N"(8×8)" pattern. After the formation of these layers, the N beam and the Al beam were turned on and an AlN layer was grown. Unexpectedly, the Al starting layer gave an AlN film with poorer orientation than the SiN starting layer. Instead of parallel epitaxy, a strong doublet structure in the LEED pattern developed indicating two slightly rotated orientations and, in addition, a weaker orientation rotated 30° with respect to the substrate. On the other hand, the SiN starting layer lead to films with only parallel orientation with short arcs in the LEED pattern indicating some

scatter about the perfect alignment. Initially, the SiN(8×8) layer was converted into AlN. Surprisingly, the three-dimensional SiN layer ("doublet structure" in the LEED literature) could also be slowly converted by the Al flux into AlN.

In all cases, the grain size was very small (<100 nm) and could neither be increased noticeably by annealing nor by deposition at the highest temperatures at which Al still was sticking. Layers of AlN showed only weak faceting in the thickness and temperature range studied.

Layers of GaN were grown on Si(111) only on AlN buffer layers without breaking vacuum. The layers continued the orientation of the buffer layer but developed pronounced faceting. No significant increase in grain size could be observed.

Growth on 6H-SiC(0001) Substrates. In order to discover whether or not the GaN grain size was determined by the small AlN grain size in the buffer layer, GaN was deposited directly on SiC, starting initially from 730°C and reducing the temperature to as low as 575°C in order to determine the optimum growth temperature. In the first experiment, a 6H-SiC(0001) crystal etched by David Larkin of NASA Lewis which exhibited flat bottom etch pits and a good LEED pattern was used. The grains in this layer were not much larger than those on the AlN buffer layer, but the faceting was more pronounced.

The next series of experiments were conducted using a SiC(0001) crystal which had a well-developed regular step structure, see Fig. 1. The surface was prepared by high-temperature hydrogen etching by Feenstra's group at Carnegie Mellon University. An excellent LEED pattern was observed (Fig. 2) after annealing at relatively low temperatures (several hundred

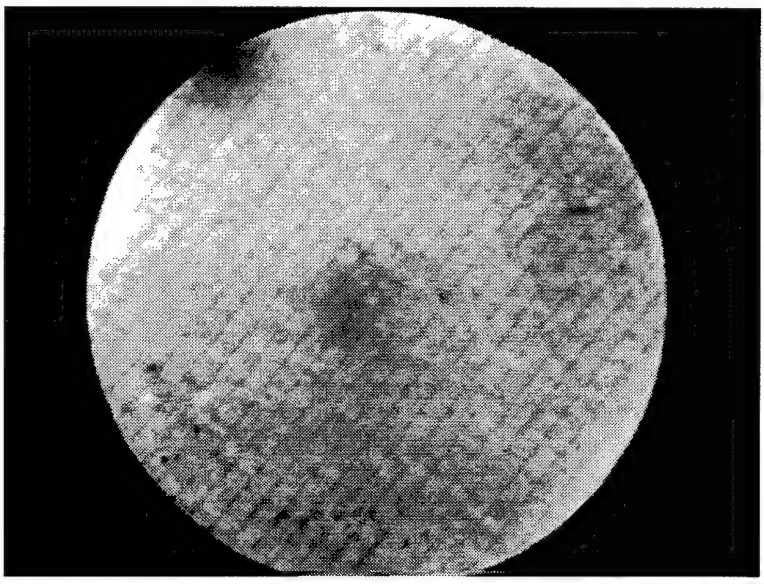

Figure 1. LEEM image of clean SiC surface. Energy 5.9 eV. Field of view 4.8 μm.

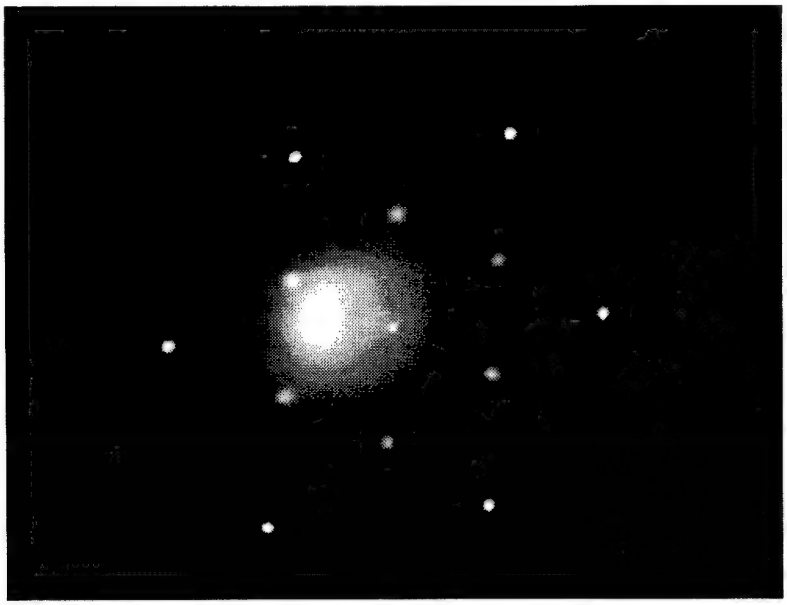

Figure 2. LEED pattern of clean SiC surface (22.8 eV).

degrees C). Figure 3 shows a sequence of images taken during the second GaN deposition after desorbing the initially deposited layer which caused some modification of the step structure as seen by comparing Fig. 1 and the first frame of Fig. 3. The deposition was made at a fixed substrate temperature (650°C). The images clearly show nucleation at the steps and growth of three-dimensional crystals which have not grown together into a continuous film at a thickness of 6 nm as determined by Auger depth profiling in a separate system after the end of the deposition. Although the crystals appear flat in the LEEM images, they show pronounced faceting in the LEED pattern.

Figure 4 shows some LEED patterns taken at different energies which show the typical movement of the facet spots with energy. They are due to (1012) facets which appear frequently in the growth of GaN crystals. It is interesting to note that the facets developed equally strongly under excess Ga flux. The strong secondary electron background in the LEED patterns (Fig. 4) was due to emission from the wide bandgap GaN film.

D. Conclusions

The experiments with the RF plasma nitrogen source have demonstrated the feasibility for the LEEM to work at reasonably high pressures. Although preliminary in nature, these results provide a good basis for the comparison with the future experiments with the supersonic seeded beam source. One problem encountered is the lifetime of the Al evaporative sources which up to now have allowed only a few depositions before the source had to be repaired. Efforts to alleviate this problem are in progress.

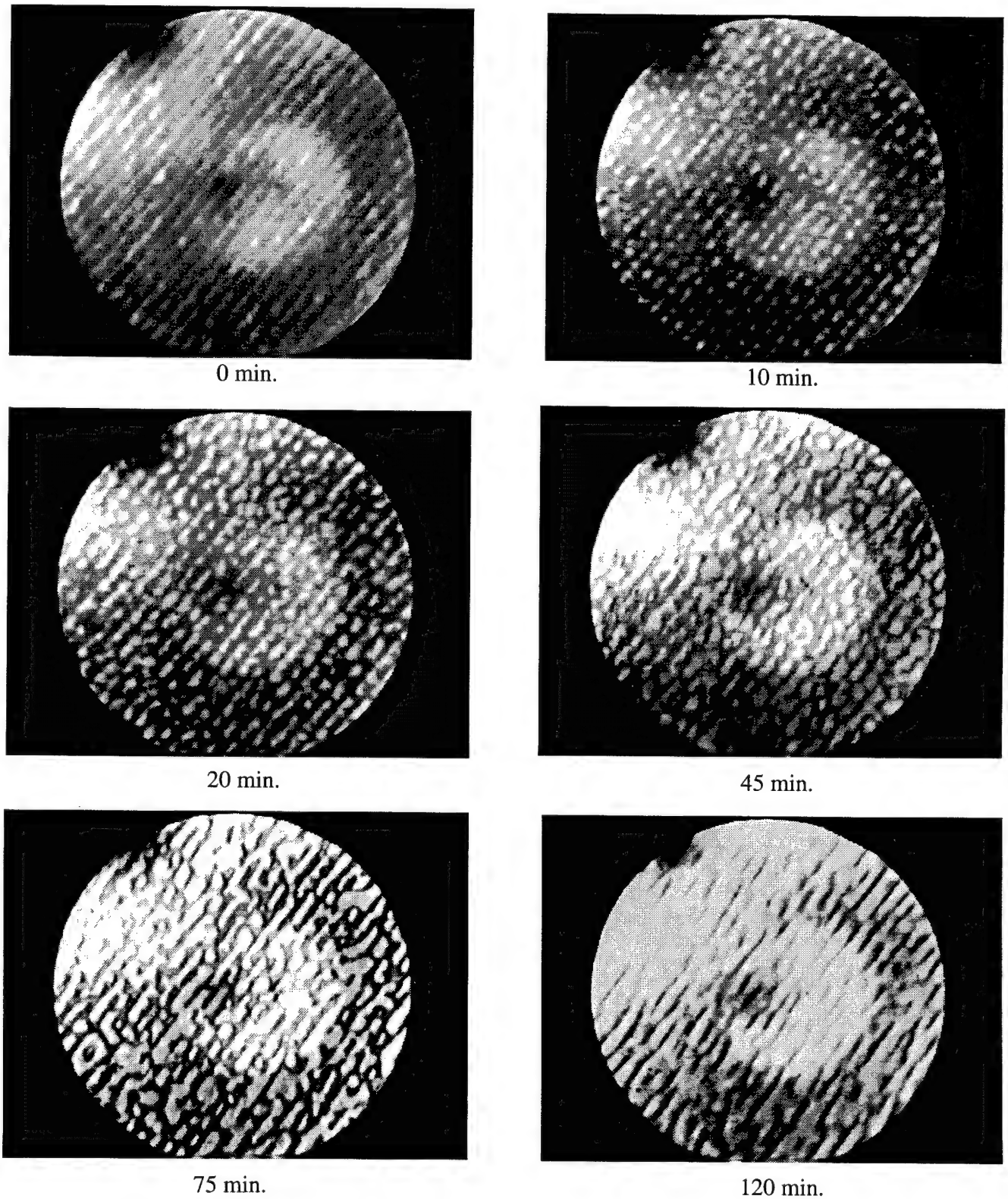

Figure 3. Growth of GaN on SiC. LEEM images taken at 6.6 eV. Field of view is 4.8 μm.

18.8 eV

16.6 eV

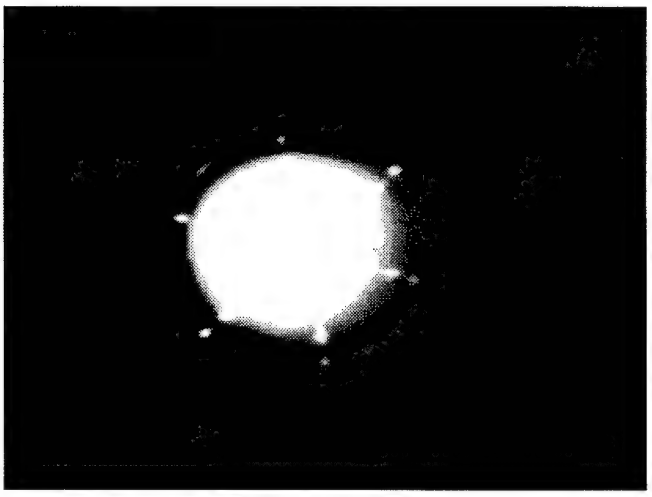

17.7 eV

Figure 4. LEED pattern of the GaN layer shown in Fig. 3, at different energies.

IV. Selected Energy Epitaxial Deposition (SEED) of III-V Nitride and SiC Thin Films

A. Introduction

Gallium nitride is a wide bandgap semiconductor (Eg=3.4 eV) with great potential for optoelectronics and high-temperature, high-frequency, microelectronics applications. Gallium nitride forms a continuous range of solid solutions with AlN (6.28 eV) and InN (1.95 eV), permitting the fabrication, via bandgap engineering, of laser diodes with tunable emission frequencies from covering the visible and UV regions. State-of-the-art GaN films ($\leq 10^8$ defects per cm^2) have been used to fabricate blue light emitting diodes (LEDs) and laser diodes.

Heteroepitaxial growth of high-quality monocrystalline GaN films has been problematic due to the lack of a suitable lattice-matched substrate and the thermodynamic instability of GaN under high-temperature chemical vapor deposition (CVD) conditions. Sapphire, the most common substrate, exhibits a 14% lattice mismatch at the GaN(0001)/sapphire(0001) interface; moreover, the thermal expansion coefficient of sapphire is 25% greater than that of GaN. Only by employing a low-temperature AlN or GaN buffer layer can one obtain monocrystalline GaN films on sapphire with defect densities in the 10^8-10^9 cm^{-2} range.

Substrate temperatures in excess of 1000°C are employed for growth of monocrystalline GaN films by halide or metal-organic CVD using NH_3. In CVD, substrate thermal energy is used to overcome activation barriers for precursor decomposition and adatom surface migration (lateral diffusion); however, GaN decomposition above 620°C *in vacuo* necessitates the use of large V/III flux ratios [1]. Plasma-assisted processes have been utilized to lower the GaN growth temperature to approximately 700°C, but ion-induced damage and oxygen contamination are often observed.

The use of energetic neutral beams of precursor molecules is an alternative approach to the epitaxial growth of GaN films at lower substrate temperatures. In selected energy epitaxy (SEE), heavy reactant molecules are seeded in a supersonic expansion of light molecules and thereby accelerated to hyperthermal energies. The precursor molecules attain kinetic energies on the order of several eV which can provide the necessary energy for activating surface processes, such as dissociative chemisorption and adatom migration. Hence, in prospect, monocrystalline GaN films may be grown at much lower substrate temperatures by SEE than by conventional thermal techniques [2]. Moreover, energetic neutral beams with narrow energy distributions are ideal means for fundamental studies of wide bandgap semiconductor growth using *in situ* low-energy electron microscopy (LEEM) and other techniques.

As discussed in the previous report (Dec. 1996), GaN thin films have been deposited at 600°C via SEE using NH_3 and TMG seeded in He supersonic molecular beams. From these results, it was evident that a two-step growth sequence involving low-temperature deposition

of a buffer nucleation layer followed by growth at higher temperatures is required to achieve smooth, highly-oriented GaN films on sapphire(0001).

To elucidate the potential advantages of SEE, homoepitaxial growth of GaN was investigated in order to better isolate the effects of precursor kinetic energy on growth kinetics and film morphology. In this report, initial results are presented of GaN homoepitaxial growth using TEG-seeded and NH_3-seeded supersonic molecular beams.

B. Experimental Procedure

The SEED/XPS multi-chamber system was described in previous reports (Jun. 1996, Dec. 1996). The orifices used in the TEG and NH_3 nozzles were 50 and 150 μm, respectively. Conical skimmers used for extracting both TEG and NH_3 beams from supersonic free jets have an opening of 1 mm in diameter, a base of 20 mm in diameter, an included angle of 25° at the opening and of 70° at the base, and a height of 17 mm. The collimation apertures of 5×5 mm^2 are located downstream between the 2nd differential pumping stage and the growth chamber. The two molecular beams are directed to the substrate with incident angles of 6° with respect to the surface normal. The deposition area on the vertical substrate is 15×15 mm^2.

The substrate is heated by radiation from a BN-coated graphite heating element to a solid Mo sample holder, as described in the previous report (Dec. 1996). In order to improve thermal contact between the Mo sample holder and the GaN or sapphire substrate, several low-vapor-pressure metals (Table I) were tried. Good temperature uniformity was obtained for temperatures <750°C using In bonding; however, In evaporation occurred readily at temperatures >800°C. When Ag paste is used, good temperature uniformity is routinely obtained for substrate temperature ≤940°C. As the substrate temperature approaches 960°C, the Ag melts resulting in evaporation and losing contact between substrate and Mo block. Gallium has a lower vapor pressure than In or Ag; however, its higher surface energy (Table I) does not allow it to wet the sapphire or SiC substrates. When Ga was tried, the initial contact between substrate and Mo block was non-uniform, and the substrate was not bonded securely. Sn appears to be an attractive alternative to Ag for the use at temperatures >940°C. Sn has a much

Table I. Estimated Surface Energies, Melting Points, and Temperatures Corresponding a Vapor Pressure of 7.6×10^{-5} Torr for Selected Metals

	Surface energy (erg/cm^2)	Melting Point (°C)	Temperature (°C) at $P=7.6\times10^{-5}$ Torr)
Mo	2445	2610	2081
In	652	157	729
Sn	926	232	977
Ag	939	962	815
Ga	1375	30	822

lower vapor pressure and a comparable surface energy to Ag (Table I); however, it has a higher melting point than In and is readily oxidized when heated in air. Consequently, Ag paste is currently used for substrate bonding, allowing a maximum substrate temperature of 920°C.

For the homoepitaxial growth of GaN, the substrates were 2-μm thick GaN films grown by MOCVD on 0.1-μm thick AlN-coated on-axis 6H-SiC, which were provided by M. Bremser of Prof. Davis' group. The GaN and AlN buffer layers were grown respectively at 1000°C and 1100°C using TEG, TEA and NH_3. The TEG and TEA flow rates were 26.1 and 23.6 μmol/min, respectively. NH_3 flow rate was 1500 sccm, and dilution H_2 flow rate was 3000 sccm.

After ultrasonic degreasing in trichloroethylene, acetone and methanol each for 5-min, 10-min etching in 1:1 HCl:H_2O at room temperature was made to prepare a clean GaN surface. The GaN substrate was then immediately dried in flowing dry nitrogen, and bonded to the Mo sample holder with Ag paste. The Mo block was then placed on a hot plate to dry the Ag paste for 5-min at 80°C.

Subsequently, the Mo block was put in the load-lock chamber, then was transferred into the deposition chamber via transfer lines. The load-lock chamber was evacuated by an Alcatel Drytel pump while the transfer lines were evacuated by a cryopump. Prior to growth, the sample was slowly heated to 400°C and maintained for 1 h under impingement of NH_3 seeded supersonic beam. After the substrate temperature was raised to growth temperature (600, 650 or 700°C) under NH_3 supersonic beam, the homoepitaxial growth of GaN was started by directing a TEG-seeded supersonic beam to the substrate, and growth was continued for 3 h. Table II shows the growth conditions for several samples.

Table II. Homoepitaxial Growth Conditions

Run	#1	#2	#3	#4	#5	#6
TEG bubbler temperature (°C)	---	10	10	10	10	10
He flow through TEG bubbler (sccm)	---	60	60	60	60	60
Stagnation pressure at TEG bubbler	---	840	840	845	920	920
NH_3 nozzle temperature (°C)	200	200	200	200	200	200
NH_3 flow rate (sccm)	20	20	20	20	60	60
He flow rate through NH_3 nozzle (sccm)	200	200	200	200	200	200
Stagnation pressure at NH_3 nozzle (Torr)	820	820	820	820	830	830
Substrate temperature (°C)	800	700	650	600	700	600

After growth, the sample was transferred to XPS (PHI) chamber through vacuum transfer lines. XPS spectra were taken with both Mg and Al anodes to resolve N(1s) signal (using Mg anode) or C(1s) signal (using Al anode) from other interferencing peaks.

C. Results and Discussion

Figure 1 shows XPS spectra of GaN/AlN/6H-SiC substrate after etching by HCl:H_2O (1:1) and after subsequent heating at 800°C under NH_3 seeded supersonic beam for 15 min in the deposition chamber. Here, O and N signals were measured using Mg anode and were normalized by the integrated intensity of Ga(3d) photoelectron peak. C(1s) and Ga(2p) signals were measured using Al anode and were also normalized by corresponding integrated intensity of Ga(3d) photoelectron peak. It is apparent that oxygen and carbon concentrations decreased after heating under the NH_3 beam at 800°C. Conversely, the Ga and N concentrations increased as the result of surface cleaning.

Figure 2 shows the O(1s), C(1s) and N(1s) and Ga(2p) XPS peaks after heating at 800°C under NH_3 flux and after GaN homoepitaxial growth under the conditions listed in Table II. The spectra in Fig. 2 were all taken with a photoelectron takeoff angle of 90° with respect to the sample surface.

The estimated Ga/N ratios after heating treatment and each growth run are given in Table III. After heating for 15 min under an NH_3 supersonic beam at 800°C, the GaN surface is nearly stoichiometric. In contrast, after growth at 700°C using TEG and NH_3 (20 sccm) seeded supersonic beams, the surface has become Ga-rich. The presence of elemental Ga is indicated by the asymmetry of the Ga(2p) peak. Concomitant broadening and distortion of the N(1s) peak are observed. Upon decreasing the growth temperature, first to 650°C and then to 600°C while holding the NH_3 and TEG fluxes constant, the N(1s) and Ga(2p) peaks narrow, and the Ga/N ratio decreases. Increasing the NH_3 flux (60 sccm) in Runs #5 and 6, leads to a further decrease in Ga/N ratio and narrowing of N(1s) and Ga(2p) photoelectron peaks. Nevertheless, the homoepitaxial films grown using the highest NH_3 flux at the lowest substrate temperature (600°C) were Ga-rich, indicating an inadequate supply of active N species during growth. The carbon and oxygen contaminations remained low irrespective of the growth conditions.

From atomic force microscopy (AFM) measurements, the growth surface was found to be faceted and the average growth rate is 20 nm/h. Further growth and characterization experiments are planned to investigate the effects of NH_3 and TEG incident kinetic energy on GaN homoepitaxy.

D. Conclusions

Homoepitaxial growth of GaN using TEG- and NH_3-seeded supersonic beams was achieved, and the films were characterized by XPS and AFM. Initial results indicate that the films are Ga-rich and exhibit a highly faceted surface morphology.

Table III. Ga/N Ratios on GaN Surface after Heating Treatment and Each Run of Growth

Run	#1	#2	#3	#4	#5	#6
Ga/N ratio	0.97	1.29	1.32	1.22	1.23	1.17

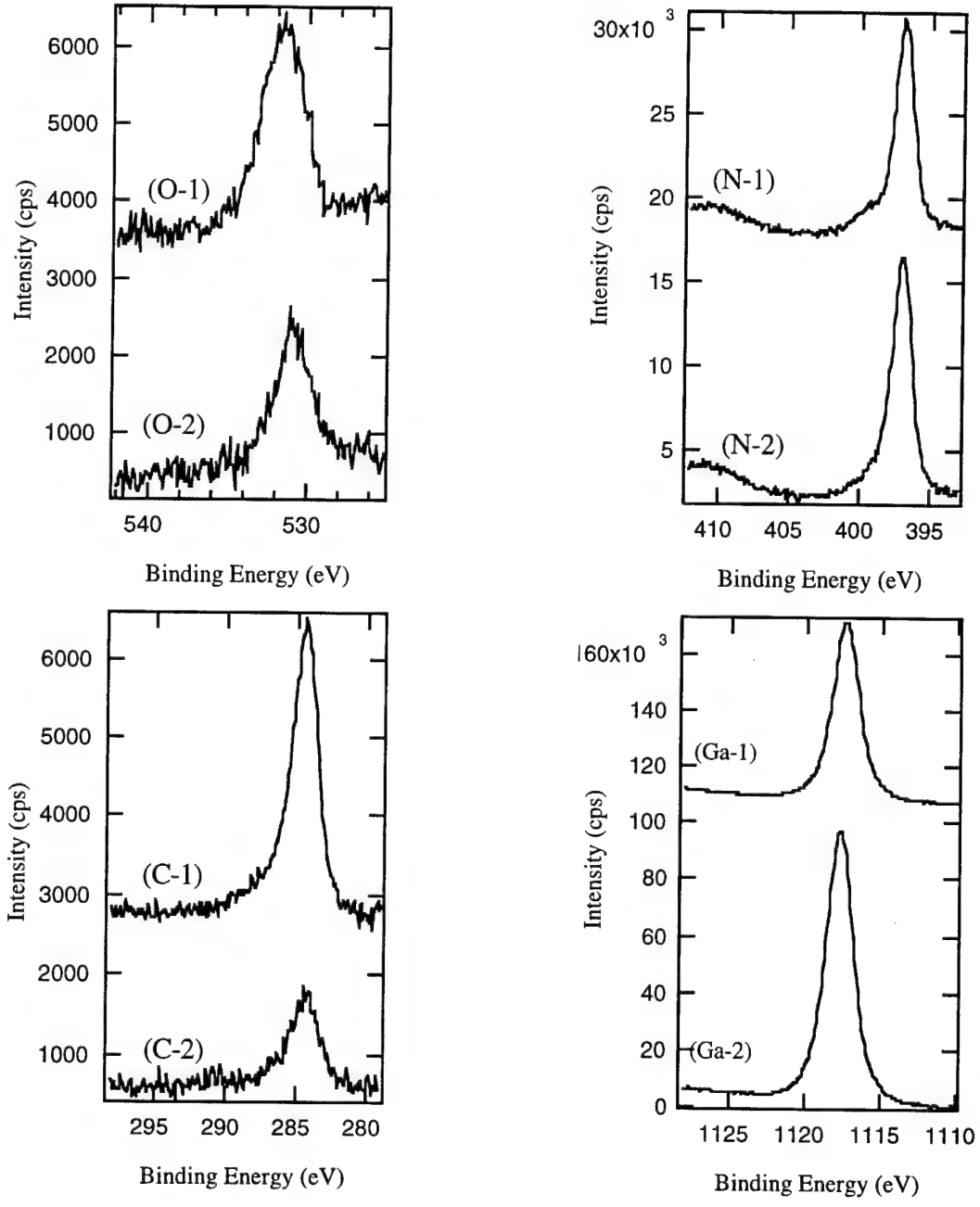

Figure 1. XPS spectra of GaN substrate after HC:H_2O etching (1) and after heat treatment at 800°C under NH_3 seeded beam for 15 min (2).

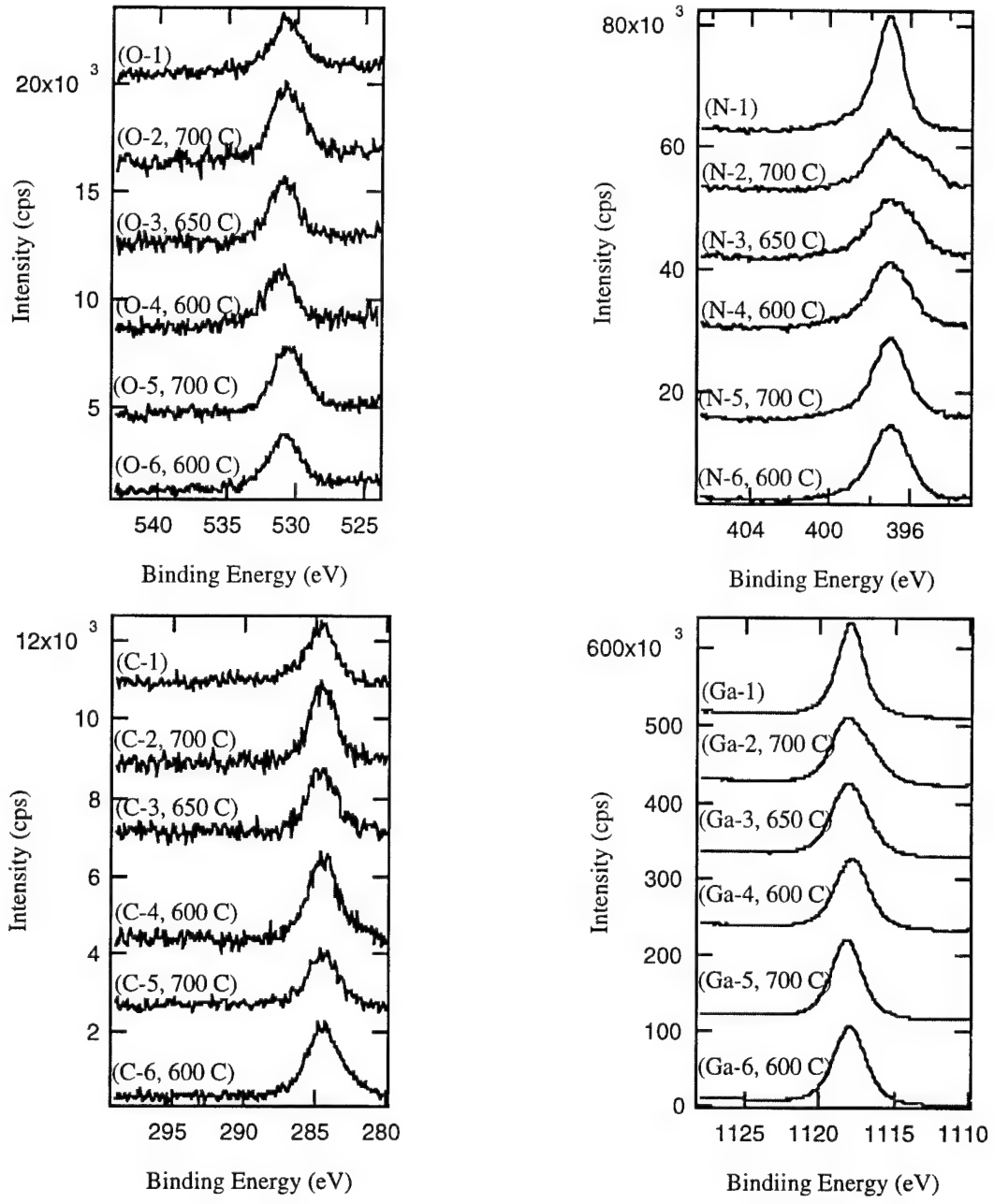

Figure 2. XPS spectra of samples after heat treatment at 800°C under NH_3 flux (1), after 3-h growth at 700°C (2), after 3-h growth at 650°C (3), after 3-h growth at 600°C (4), after 3-h growth at 700°C (5) and after 3-h growth at 600°C. NH_3 fluxes were 20 sccm for (2) through (4), and were 60 sccm for (5) and (6).

E. Future Plans

Future plans include: 1) a detailed investigation of GaN homoepitaxial growth to reveal the relationship between film quality and molecular kinetic energies tuned by supersonic beams, 2) a new gas line for generating TEA (Triethylaluminum) supersonic beam will be installed to grow AlN buffer layers on sapphire and 6H-SiC substrates, 3) a gallium effusion cell (K-cell)

will be installed, as well, to grow GaN with Ga effusive beam and NH_3 seeded supersonic beam, and 4) comparison of homoepitaxial and heteroepitaxial growth results and comparison of results using Ga effusive molecular beam and TEG supersonic molecular beam to draw conclusions on the advantages of selected energy epitaxial deposition using supersonic molecular beams.

F. References

1. S. Nakamura, Japan. J. Appl. Phys. **30**, L1705 (1991).
2. M. R. Lorenz and B. B. Binkowski, J. Electrochem Soc. **109**, 24 (1962).

V. Transmission Electron Microscopy of GaN and AlN Films Grown on 6H-SiC(0001) via NH_3-seeded He Supersonic Molecular Beams

A. Introduction

The nitride family of AlN, GaN and InN thin films have shown to be strong candidates for electronic and optoelectronic applications. With direct band gaps of 6.2 eV, 3.4 eV and 1.9 eV for AlN, GaN and InN respectively, solid solutions based on these materials provide for band gap modifications suitable for applications ranging from the red to the deep UV region of the spectrum [1]. Due to the high bond strength between N and H in NH_3, the growth of III-V nitrides requires high substrate temperatures unless some other form of activation is present. Supersonic molecular beam epitaxy (SMBE) has been shown to enhance the surface decomposition of silane and methane [2,3] because of the possibility of tuning the kinetic energy of these species to deform and cleave the bonds upon impact with the substrate. In addition, the tuning of the energy spread is possible with SMBE. This is important in order to experimentally determine the chemisorption barriers for the systems being studied, as well as to provide species with high sticking coefficients at high enough intensities. Supersonic molecular beam epitaxy is, therefore, a useful technique for the low-temperature growth of single-crystalline GaN films at suitable growth rates using NH_3. A review of supersonic molecular beams can be found in Scoles [4].

AlN and GaN films grown using NH_3-seeded He SMBE were characterized via transmission electron microscopy (TEM).

B. Results and Discussion

Figure 1 shows a TEM micrograph of the GaN/AlN/SiC structure with a selected area electron diffraction pattern (SAEDP). The SAEDP of the GaN/AlN/SiC structure showed distinct SiC, AlN and GaN diffraction spots. The high order diffraction spots and the lack of streaking confirmed that the films were crystalline and well ordered. The estimated thickness of the AlN buffer layer and GaN layer were 65 nm and 106 nm, respectively. The GaN layer had a defect density of $2\times10^{10}cm^{-2}$ and the AlN buffer layers contained a higher defect density of at least an order of magnitude.

The AlN/SiC interface was clean and coherent as examined at high magnification using TEM (Fig. 2). The ..abc-bac.. hexagonal stacking sequence of SiC followed by ..ab-ab.. stacking for AlN aligned along the (0001) direction was clearly resolved. This image confirmed the excellent epitaxial relationship between the AlN film and the SiC substrate. Planar defects originated at the SiC steps and ran into the AlN films. These defects were identified as interface domain boundaries (IDBs) [5].

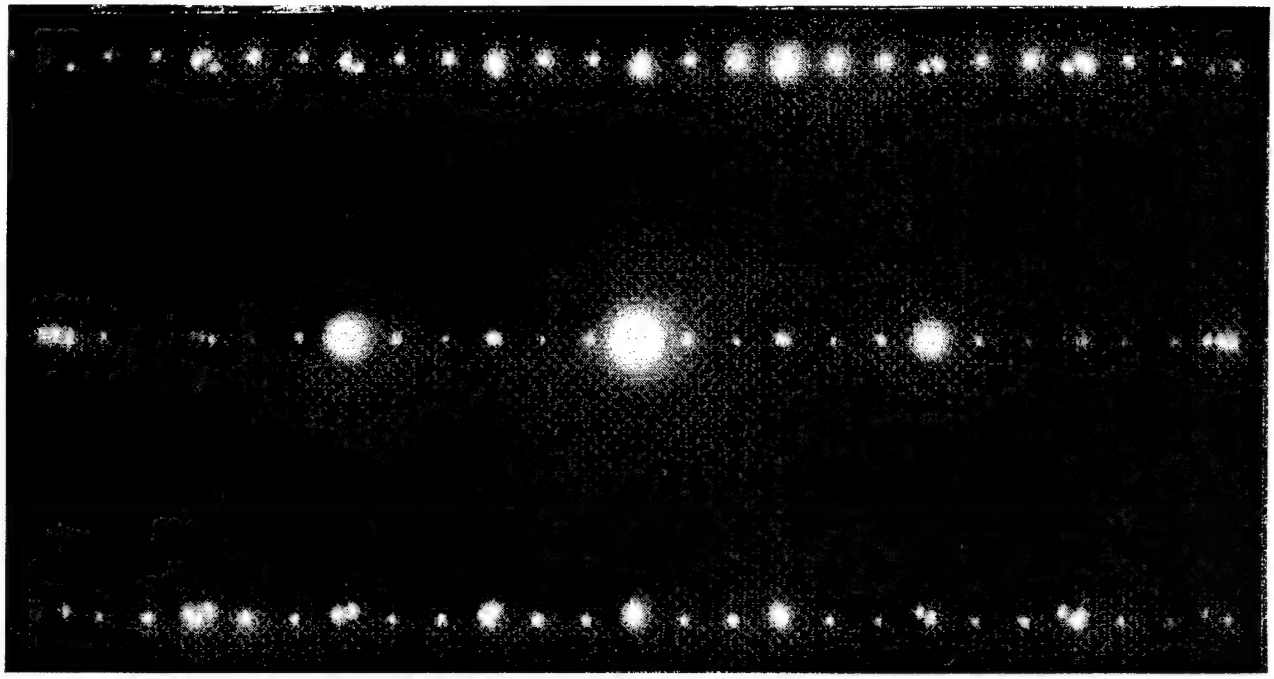

a)

b)

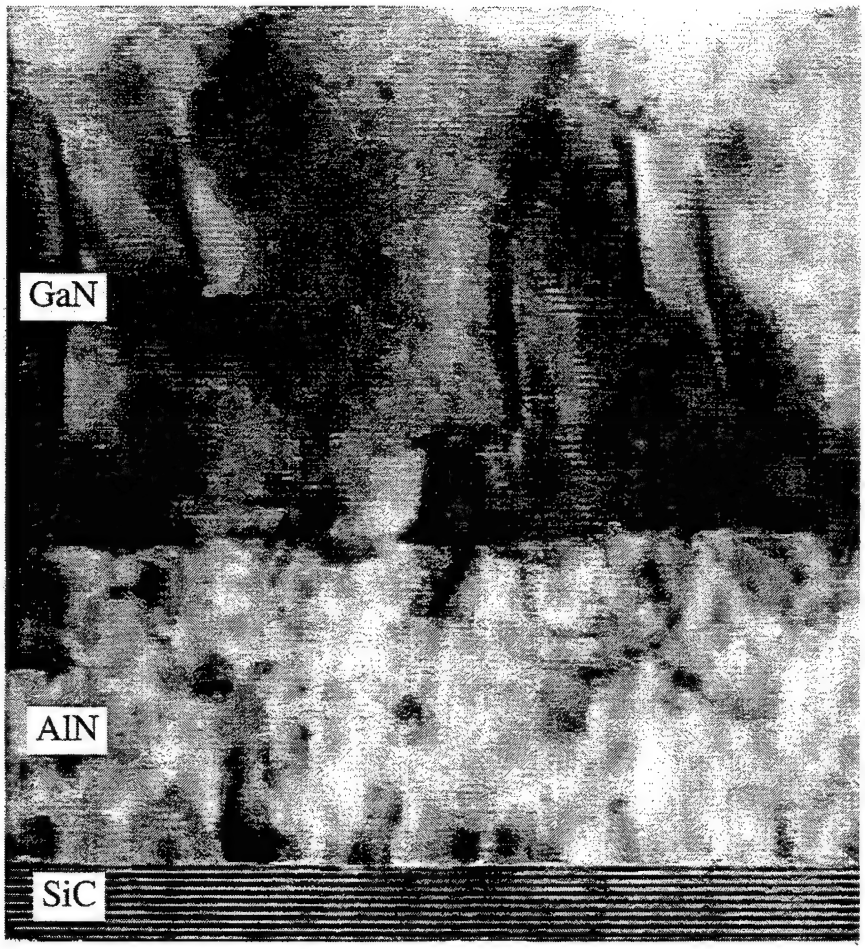

Figure 1. a) Selected area electron diffraction pattern of the GaN/AlN/SiC structure, b) electron micrograph of the GaN/AlN/SiC structure.

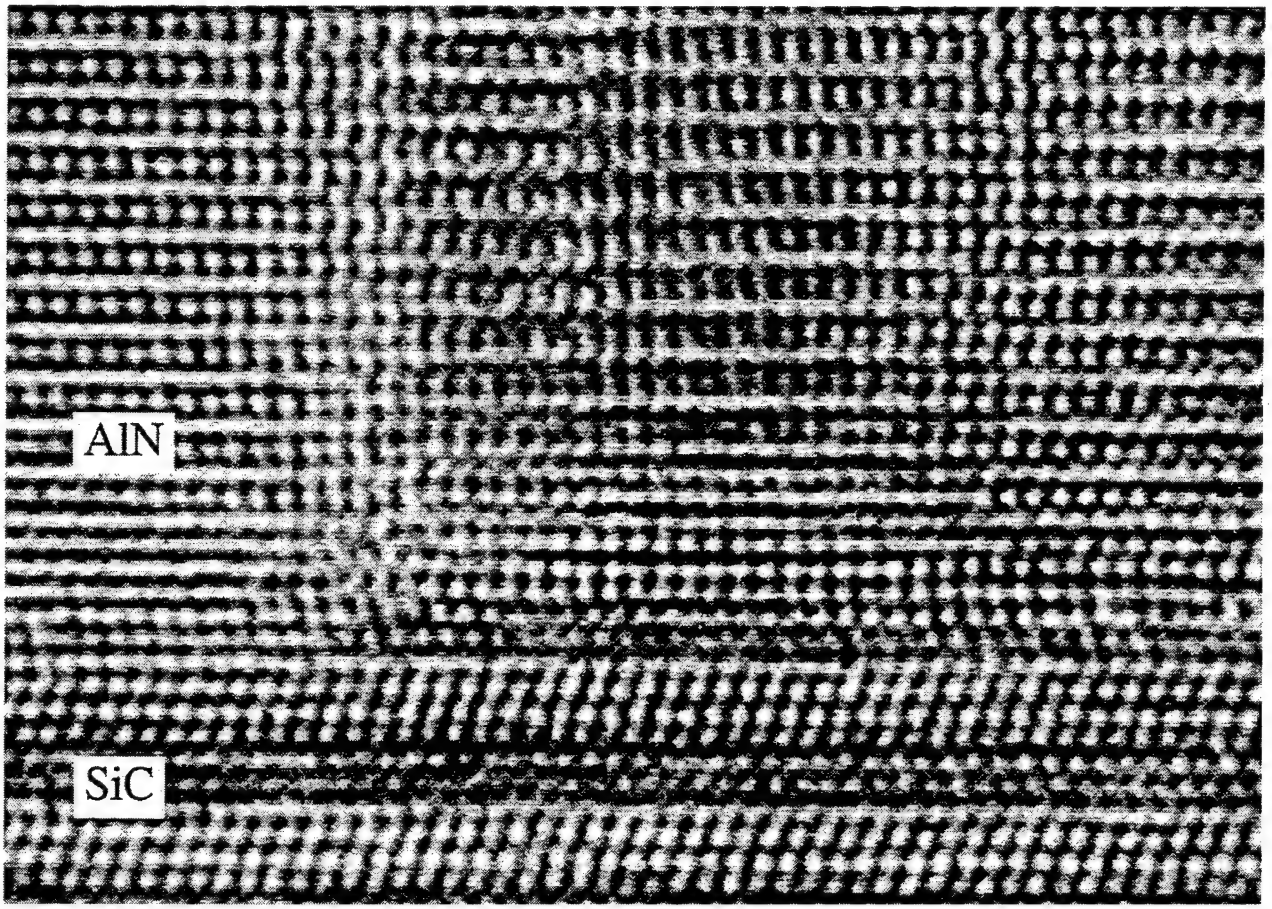

Figure 2. High resolution electron micrograph of the AlN/SiC interface.

By comparing the NH_3 beam intensity ($\approx 3\times10^{14}$ $cm^{-2}s^{-1}$) with the GaN film thickness, it was estimated that 41% of the NH_3 impinging on the film surface was incorporated in the film. The beam intensities were measured by the Pitot technique with an ion gauge in direct line of sight with the beam. This geometry gave an over estimate of the beam intensity. Therefore, the true N incorporation was greater than 41%. Kim *et al.* [6] used a thermal beam of NH_3 with an intensity of 5.53×10^{15} $cm^{-2}s^{-1}$ and obtained growth rates of $\approx$ 1.1 μm/h which yield a N incorporation of 23%. Similar results were obtained by Yang *et al.* [7].

C. Conclusion

TEM analysis of AlN films on off axis 6H-SiC(0001) and subsequent GaN layers grown using NH_3 seeded He supersonic molecular beams were conducted. The GaN films were epitaxial with a thickness of $\approx$0.1μm and a defect density on the order of $2\times10^{10}cm^{-2}$ while the AlN buffer layers contained about an order of magnitude higher defect density relative to GaN. N incorporation efficiencies greater than 41% are possible using NH_3 kinetic energies of 0.40 eV during GaN film growth.

D. Future Work

The SMBE chamber has been connected to the LEEM and aligned. In the next three month period, real-time LEEM observations on GaN growth by the SMBE method will be conducted.

E. References

1. S. Strite and H. Morkoc, J. Vac. Sci. Technol. **B10**, 1237 (1992).
2. M. E. Jones, L. Q. Xia, N. Maity, J. R. Engstrom, Chem. Phys. Lett. **229**, 401 (1994).
3. S. T. Ceyer, J. D. Beckerle, M. B. Lee, S. L. Tang, Q. Y. Yang, M. A. Hines, J. Vac. Sci. Technol. A **5**, 501 1987).
4. D. R. Miller, Atomic and Molecular Beam Methods, Ch. 2, Ed. G. Scoles, Oxford University Press (1988).
5. R. F. Davis, S. Tanaka and R. S. Kern, J. Cryst. Growth **163**, 93 (1996).
6. W. Kim, O. Aktas, A. E. Botcharev, A. Salvador, S. N. Mohammad and H. Morkoc, J. Appl. Phys. **79**[10], 7657 (1996).
7. Y. Yang, L. K. Li and W. I. Wang, J. Vac. Sci. Technol. B **14**[3], 2354 (1996).

VI. Arc-Heated Supersonic Free-Jet of Nitrogen Atoms for the Growth of GaN, AlN and InN Thin Films

A. Introduction

Molecular beam energies in the 1960's could be classified into two categories: (i) energies below 1 eV produced by oven-heated sources and (ii) energies above 20 eV generated by ion beam sources. The upper limit of the former method is given by the melting temperature of the oven material and produces, therefore, a beam with a broad energy spectrum, while the lower limit of the latter technique is determined by the electrostatic repulsion of the ions, which leads to lower beam intensities. As suggested by Fenn and Anderson [1], a combination of a supersonic expansion, utilizing the narrow energy distribution, and the seeding of a heavier species into a light carrier gas leads to the availability of a high-energy, heavy-particle beam with narrow energy distribution. Young *et al.* [2] combined this technique with a high-temperature arc-heated jet to generate an Argon beam of energies up to 21 eV. Bickes *et al.* [3] then seeded nitrogen into argon to produce an atomic nitrogen beam with intensity $>10^{17}$ atoms/sr/sec. These high-intensity, high-energy beams were used in the 1970's and 1980's for crossed molecular beam scattering experiments. In this decade, they seem to offer the opportunity for employment of III-V nitrides growth.

B. Experimental Procedure

The arc-heated jet source, shown in Fig. 1, was constructed and then tested in the supersonic molecular beam epitaxy chamber described in previous reports and tested under various conditions. A premixed 8% nitrogen in argon was used for these tests. Two very distinct working modes of the arc were found: an internal mode and an external mode. The "internal arc" is characterized by an intense white glow on the inside of the assembly and has a low arc voltage, U<2V and I=40-125A. The "internal arc" is readily obtained by drawing the

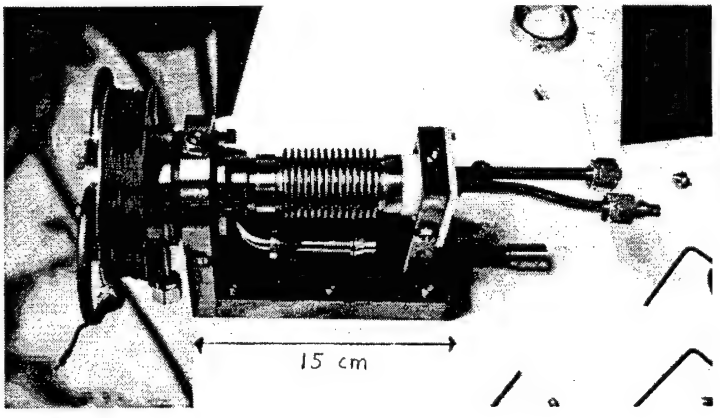

Figure 1. Arc-heated jet source.

arc, i.e., by bringing cathode and anode in contact, applying the arc current and then drawing the cathode back carefully.

Since the plasma of the arc is inside the assembly, this mode is most often accompanied by heavy electrode erosion. Furthermore, no atomic nitrogen could be detected by a residual gas analyzer (RGA). In contrast to what Bickes *et al.* [3] reported, it was found virtually impossible to convert the "internal arc" to an external one by merely increasing the stagnation pressure, instead the arc just broke off.

The "external arc" is characterized by an intense blue-purple plasma plume standing outside the nozzle of the source with higher arc voltage, U=10-15V and I=60-100A, see Fig. 2. The "external arc" was established in two different ways: first, by discharging a Tesla coil across the electrode gap, where the electrode gap varied from 0.3mm to 0.4mm, and second, by having the electrodes separated initially and then bringing in the cathode with extreme caution until the arc establishes itself. The former method is more easily done, however, it also poses the danger of the arc being generated in the back of the assembly instead of the nozzle, which can cause significant melting erosion to the assembly if not turned off immediately.

The establishment of the "external arc" is non-trivial, but once the arc is formed it is effortlessly maintained for several hours. The longest running time was 2 hours and was limited by external time constraints and was not due to instabilities of the arc. The "external arc" was run at two different stagnation pressures of 650 Torr and 900 Torr, resulting in source chamber pressures of ca. 1.5×10^{-1}, the latter leading to a more rapid anode erosion than the former. The tungsten nozzle, which had a diameter of 1.25 mm, of the anode sustained heavy erosion damage by the "external arc" and can be used only a few times depending on the stagnation pressure and run time. Once the extent of erosion by the arc to the tungsten nozzle was recognized, diamond burs, usually used to polish gems, were purchased, so that it is possible now to produce these nozzles at very low cost (< $15/ piece) and in various shapes. EDM graphite skimmers were also successfully tested, after the exposure to the plasma plume of ca. 6 hours, no apparent damage to the sharp orifice edge could be found encouraging further applications. Furthermore, a self-wound electromagnet improved the stability of the arc and the glow discharge substantially.

C. Results and Discussion

Table I is a list of the partial pressures measured by the RGA and corrected for the individual ionization sensitivities.

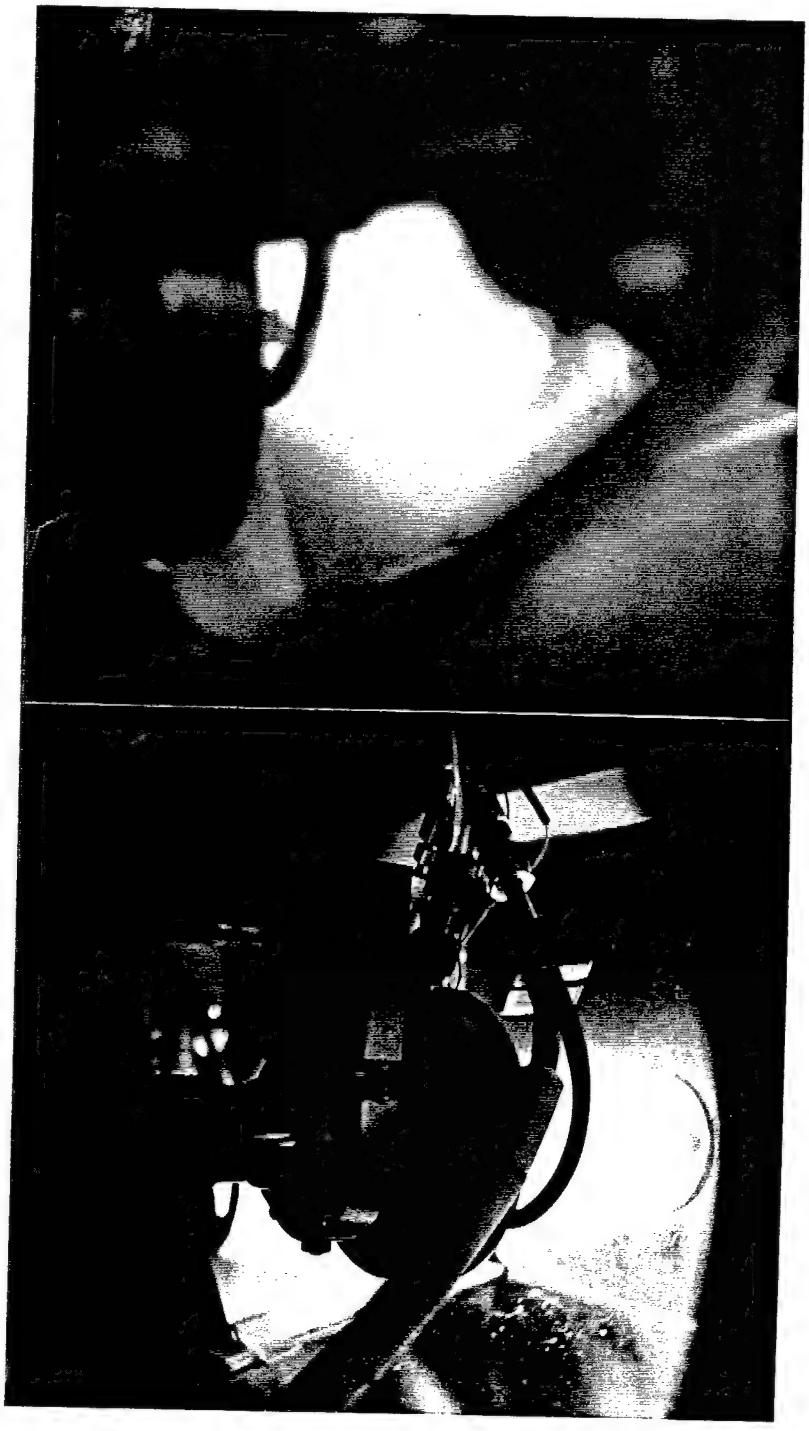

Figure 2. Views from the rear of the nozzle. The jet flow is from nozzle at left toward skimmer in circular mounting plate at right. The bright light of the "external arc" is readily discernible.

Table I. Partial Pressures

mass detected m/e	40	28	14
arc on (Torr)	$(4.48 \pm 0.08) \times 10^{-8}$	$(1.92 \pm 0.60) \times 10^{-9}$	$(2.00 \pm 0.10) \times 10^{-8}$
arc off (Torr)	$(7.47 \pm 0.03) \times 10^{-8}$	$(5.11 \pm 0.004) \times 10^{-9}$	$(1.15 \pm 0.06) \times 10^{-10}$

For each measurement, 120 data points were sampled in 1sec intervals. The fractional dissociation can be calculated from these partial pressure measurements using Bickes' approach [3],

$$\alpha = \frac{\frac{1}{2} P_N}{\left(P_{N_2} + \frac{1}{2} P_N \right)},$$

where P_N is the partial pressure of atomic nitrogen and P_{N_2} is the partial pressure of molecular nitrogen. Using the values in Table I, the fractional dissociation can be found as $\alpha = 84\% \pm 9\%$.

From the partial pressure drop of argon the temperature of the plasma plume can be extracted in the following way. The mass flow rate out of the expanding nozzle is given by

$$\dot{N} = A \frac{p_0 d^{*2}}{\sqrt{T}},$$

where p_0 is the stagnation pressure, d^* the effective nozzle diameter, and $A = 1.967 \times 10^{-4}$ is a constant for the argon/nitrogen mixture, resulting in a specific argon partial pressure. The reduced argon partial pressure, due to heating of the arc, can then be used to find an effective mass flow rate from which the temperature is calculated as follows:

$$T_{eff} = \frac{A^2 p_0^{\,2} d^{*4}}{\dot{N}_{eff}} .$$

The argon temperature is then determined to be $T = (7590 \pm 910) K$, which is somewhat lower than Bickes' results under similar conditions, but their results were based on time-of-flight (TOF) measurements, and are more precise than the mass flow evaluations.

D. Conclusion

Conditions to obtain an "external arc" in a reproducible fashion were found. Preliminary calculations of the fractional dissociation of the nitrogen, $\alpha = (84 \pm 9)\%$, and the argon

temperature, $T = (7590 \pm 910)K$, were found and agree mostly with previous experiments of Bickes [3] and Tabayashi [4].

E. Future Work

Further evaluation of the source under various conditions, such as different electrode gap, different stagnation pressures, different nozzle diameters and a bias potential between the skimmer and the nozzle has to be done. Time-of-flight measurements need to be done on the arc-heated jet to determine the energy of the atomic nitrogen beam, and to further test the graphite skimmers. Pitot measurements will give information about the intensity of the beam, this source will then be used for the growth of III-V nitrides, and to test the relative advantage of using excited molecular nitrogen versus atomic nitrogen.

F. References

1. J. B. Anderson and J. B. Fenn, Phys. Fluids **8**, 780 (1965).
2. W. S.Young, W. E.Rogers and E. L.Knuth, Rev. Sci. Instrum. **40**, 1346 (1969).
3. R. W. Bickes, K. R. Newton, J. M. Herrmann and R. B. Bernstein, J. Chem. Phys **64**, 3648 (1976).
4. K. Tabayashi, S. Oshima and K. Shobatake, *Proc. 14th International Symp. on Rarefied Gas Dynamics*, Tokyo 1984, 635.

VII. Dual Colutron Ion-beam Deposition

In our last quarterly report (December 1996), we have shown the energy ditribution of N_2^+ and N^+ ions at energies around 20 eV with FWHM of ~1 eV from one of our Colutron ion-beam systems. We have now extracted mass-selected Ga^+ ions from the second Colutron producing beams at around 14 eV with a FWHM of ~1 eV (see Fig. 1). In the next 3-month period, we will use the monoenergetic and mass-selected Ga^+ and N_2^+ ion beams for nitride film deposition on Si(111) and 6H-SiC(0001) substrates.

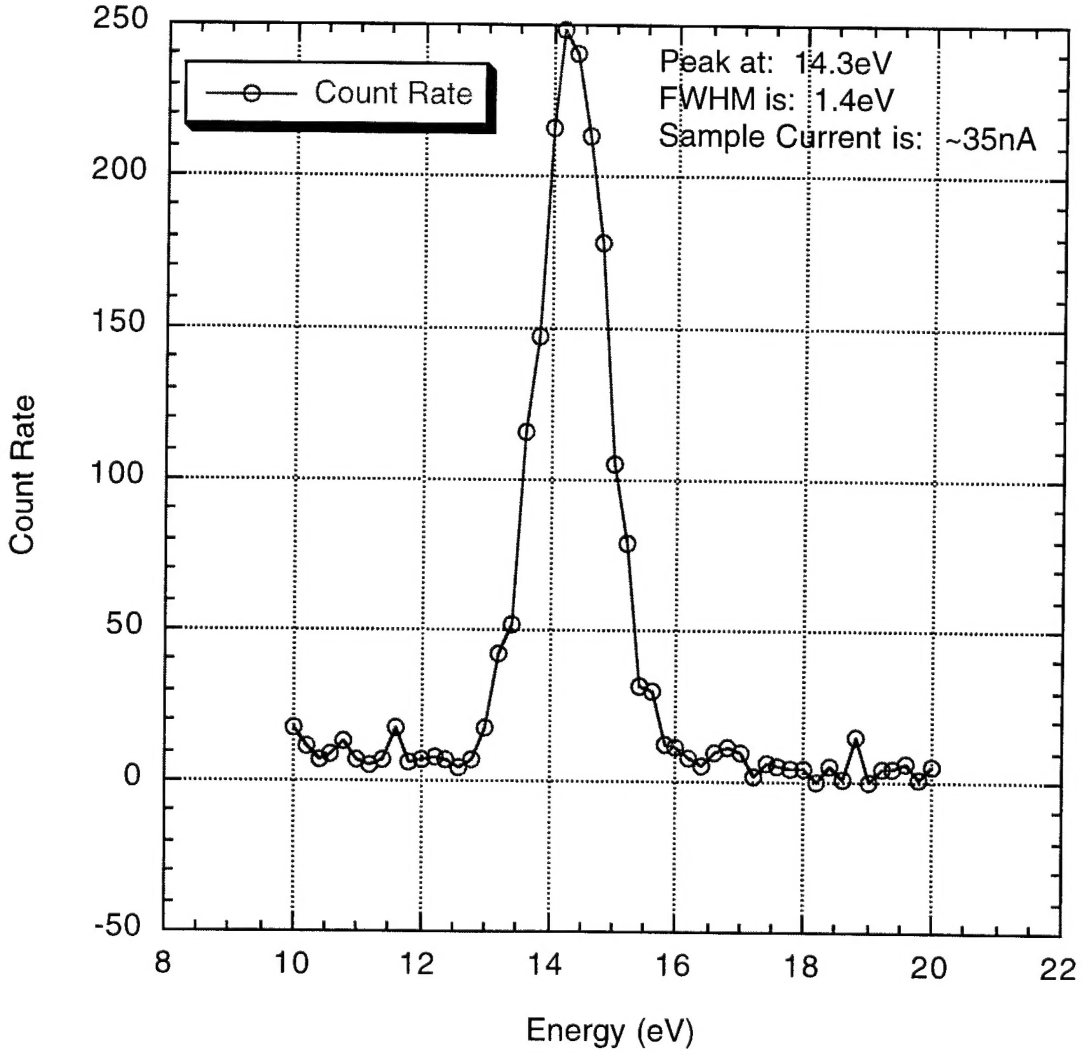

Figure 1. Energy distribution of Ga^+ ions from the Colutron ion source.

VIII. Distribution List

Dr. Colin Wood Office of Naval Research Electronics Division, Code: 312 Ballston Tower One 800 N. Quincy Street Arlington, VA 22217-5660	3
Administrative Contracting Officer Office of Naval Research Regional Office Atlanta 101 Marietta Tower, Suite 2805 101 Marietta Street Atlanta, GA 30323-0008	1
Director, Naval Research Laboratory ATTN: Code 2627 Washington, DC 20375	1
Defense Technical Information Center 8725 John J. Kingman Road, Suite 0944 Ft. Belvoir, VA 22060-6218	2